SIMULATIONS OF THE BEAM LOSS MONITOR SYSTEM FOR THE LCLS UNDULATOR BEAMLINE*

J. C. Dooling†, W. Berg, A. Pietryla, and B.-X. Yang, ANL, Argonne, IL 60439, USA
H.-D. Nuhn, SLAC National Accelerator Laboratory, Menlo Park, CA, 94025, USA

Abstract

Simulations of the beam loss monitor (BLM) system built at the Advanced Photon Source (APS) for the Linear Coherent Light Source (LCLS) have been carried out using the Monte Carlo particle tracking code MARS. Cherenkov radiation generated by fast electrons in the quartz radiator of the BLM produces the signal used to estimate beam loss and dose in the LCLS undulator magnets. The calibration of the BLM signal with radiation components that cause undulator damage is the goal of the simulation effort. Beam loss has been simulated for several scenarios including undulator magnets in the normal operating position, rolled-out 80 mm from the beamline, and absent altogether. Beam loss is generated when an electron bunch strikes one of two targets: Al foil or carbon wire. In the former case, the foil is placed at OTR33, 85.8 m upstream of the FEL; in the latter, the first undulator beam finder wire (BFW01) position is used just upstream of the first magnet. The LCLS MARS model includes quadrupole focusing between OTR33 and the end of the FEL. The FODO lattice leads to complex loss patterns in the undulators consistent with betatron envelope maximums in both transverse planes.

INTRODUCTION

Along with a high quality electron beam, magnetic fields of the LCLS undulator dipoles generate hard x-ray laser light. We know that bremsstahlung radiation created by energetic electrons can lead to degradation of these fields. The ceramic permanent magnets (PMs) are suseptible to demagnetization when subjected to various components present in the bremsstrahlung shower. To model this shower, the Monte Carlo, particle-matter interaction program MARS is employed. MARS [1] is used to simulate the bremsstrhahlung shower in both the magnets and the beam loss monitor (BLM) material. The BLM detects the shower by sampling a portion of its electrons. Highly relativistic electrons pass through the BLM radiator emitting Cherenkov radiation. The radiator material is composed of fused-silica (or synthetic quartz), which can withstand radiation doses in excess 10^8 Rads without darkening [2].

In addition to providing detectors for the machine protection system (MPS) throughout the 132-m length of undulators, the BLMs are also tasked with yielding dosimetry data for the magnets [3]. In this way, absorbed dose in the undulator magnets can be tracked over time. It is known that neutrons, and in particular, fast neutrons can demagnetize ceramic PM [4]; however, regions in the magnets where damage occurs usually do not match the overall neutron fluence. Typically, the neutrons spread out over the volume of the magnets; whereas, electron fluence peaks more closely to the beam.

MODELING WITH MARS

Two radiation sources were examined with MARS: first, scattering from an optical transition radiation (OTR) foil located roughly 85.8 m upstream of the undulators, and second, scattering from a beam finder wire (BFW) located just ahead of the first BLM. The OTR foil, designated OTR33, is composed of 1 μm of Al, whereas the BFW is a 40-μm-diameter C wire. Cross-sections of the BLM used in the simulations are presented in Fig. 1. The figure also shows the location of a tungsten (W) enhancer used to increase the number of electrons seen by the BLM radiator. A cross-sectional view in the undulator region is shown in Fig. 2.
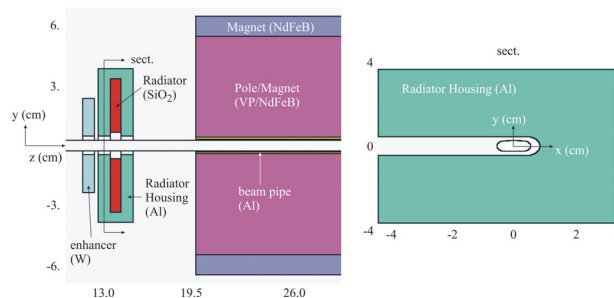
Figure 1: BLM radiator and housing and their positions with respect to the undulator magnets; two views are shown.

ANALYSIS

The energy dependence of the Cherenkov radiation in the BLM is weak; however, it is still necessary to examine the spectrum and remove electrons below the energy cutoff for the analysis. MARS provides the spectra of radiation components including electrons, photons, and neutrons. An example of electron spectra simulated within the fused-silica radiator with and without the presence of the tungstren enhancer is presented in Fig. 3. Note how the tungsten tends to soften the electron spectrum, increasing the fluence at lower energies.

Instrumentation
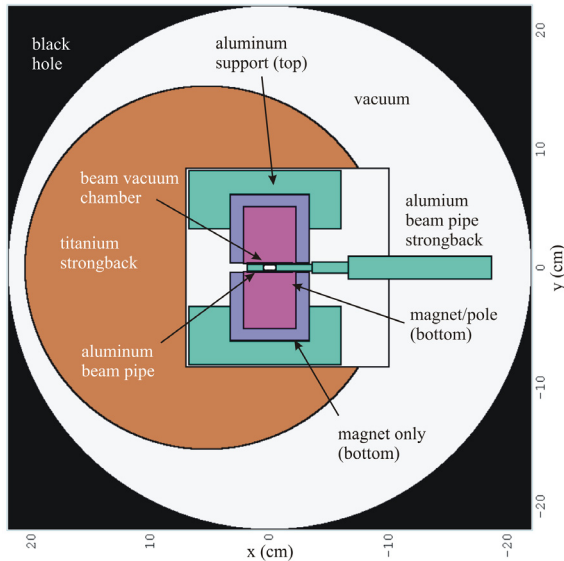
Figure 2: Undulator magnet cross section used in MARS.
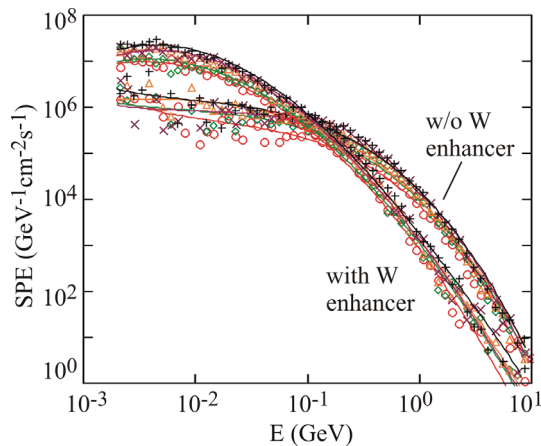
Figure 3: Electron radiator spectra at positions 7, 13, 19, 25, and 31 along the undulators with and without the presence of a W enhancer just upstream of each radiator. Undulator quadrupole fields are not present in this simulation.

BLM Signal

The BLM signal is determined from the number of Cherenkov photons generated in the radiator. The number of photons can be calculated using the Frank-Tamm formula, which can be reduced to [5],

$$\frac{N_p}{dx} = N_o(\omega_2, \omega_1)\left[1 - \frac{1}{n^2\beta^2}\right], \qquad (1)$$

where

$$N_o(\omega_2, \omega_1) = \frac{\mu}{4\pi}e^2\frac{(\omega_2 - \omega_1)}{h}. \qquad (2)$$

For ω in the optical range of frequencies defined by λ_1=600 nm and λ_2=150 nm,

$$N_o = 2.35 \times 10^3 \left\{\frac{photons}{cm}\right\}. \qquad (3)$$

Spectral fluence simulation data are most conveniently viewed and fit on a log-log scale. In the following expression, a polynomial of order 3 is chosen,

$$f_{se}(E) = \exp\left[a_o + a_1 lnE + a_2 ln^2E + a_3 ln^3E\right]. \qquad (4)$$

Examples of fit spectra were given in Fig. 3. Simulations with EGS4 have shown that electrons must possess energies of 4 MeV and above to pass completely through the radiator and its aluminum housing. Because of this requirement, the second term of Eq. 1 varies by less than 4 percent from its ultra-relativistic value of $1 - 1/n^2$=0.537 for n=1.47; therefore, the energy variation of the second term is ignored and the ultra-relativistic value is used. To obtain the number of photoelectrons generated by the photocathode, we can write

$$N_{pe} = \int_{E_{min}}^{E_{max}} dE \frac{dN_p}{dx}\eta_c\bar{\eta}_Q V_{rad}$$

$$\approx \eta_c\bar{\eta}_Q \frac{dN_p}{dx}V_{rad}\int_{E_{min}}^{E_{max}} dE f_{se}(E), \qquad (5)$$

where η_c and $\bar{\eta}_Q$ are the optical coupling and the average PMT quantum efficiencies over the wavelength range, respectively, and V_{rad} is the volume of the radiator.

Beam Optics

MARS has shown the importance of including the effects of quadrupole focusing in the simulation of the bremsstrahlung shower. Though the shower is composed primarily of photons, the interaction of the electrons with either the OTR33 foil or the BFW introduces additional divergence ($\approx 1/\gamma$) to the beam electrons. The divergence would cause additional losses over the span of the undulators without the quadrupole fields; with the quadrupole fields in place, the scattered beam loss is greatly reduced. Initial estimates of beam loss had been made without considering the quadrupole fields [6]. As will be shown below, the alternate gradient focusing has consequences on the localization of beam losses.

BEAM LOSS SIMULATIONS

Simulations were first conducted modeling the bremsstrahlung shower from OTR33 in the linac-to-undulator (LTU) beamline, 85.8 m upstream of the first undulator. To improve statistics, the density of the foil was increased by two orders of magnitude, however no dose enhancement was used in the BFW simulations. In all cases, 1-nC of 13.64-GeV, primary electrons were modeled with 10^7 macroparticles. All contour plots in this

section present fluences using $\log_{10}$ scaling. A view of the y-z electron fluence resulting from an OTR33 shower is shown in Fig. 4. Examining more closely the end of the undulators, one observes a region of beam loss in the y-z plane. This location is expanded in Fig. 5.

An example of the BFW halo is given in Fig. 6 for a beam strike on BFW01; again the view is in the y-z plane. Whereas the electron fluence is concentrated near the beam axis, the neutron fluence tends to be more spread out. Figure 7 presents neutron fluence simulation results over the same range given in the previous plot.
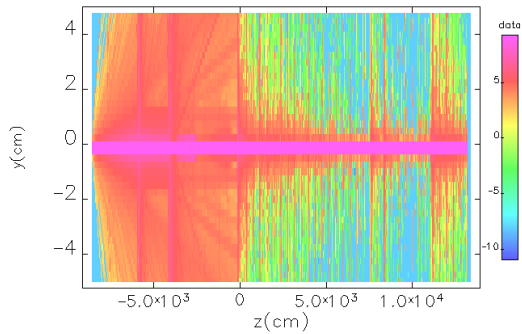
Figure 4: Electron fluence in the y-z plane integrating over the horizonal region of the undulators. The simulation region begins with the OTR33 location and includes the full length of the undulators.
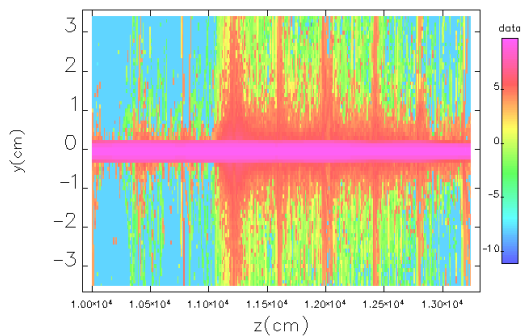
Figure 5: Electron fluence in the y-z plane near the end of the undulators. An area of elevated beam loss is noted; in addition, the losses exhibit a repeating pattern.

Finally, the usefulness of the BLM as a dosimeter for the magnets is explored. In Fig. 8, comparison is made between the peak dose in the magnets and the expected BLM signal. The signal is determined for an R7400U-04 PMT biased to 600 V and $\eta_c = 2.3 \times 10^{-4}$. Though somewhat noisy, the data, taken from a single simulation, suggests that BLM dosimetry may be possible.

REFERENCES

[1] N. V. Mokhov and S. I. Striganov, "MARS15 overview," Tech. Rep. Fermilab-Conf-07/008-AD, 2007.
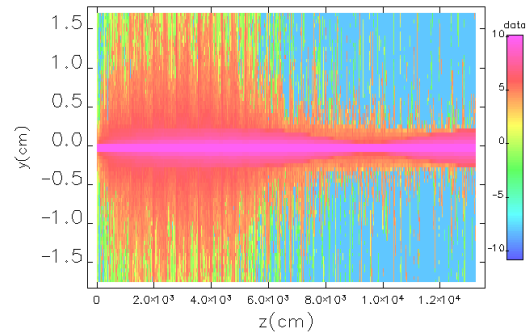
Figure 6: Undulator electron fluence in the y-z plane for a BFW01 beam strike.
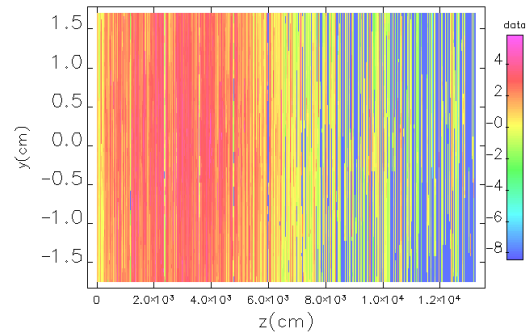
Figure 7: Neutron fluence in the y-z plane covering the same region as Figure 6 for a BFW01 beam strike.
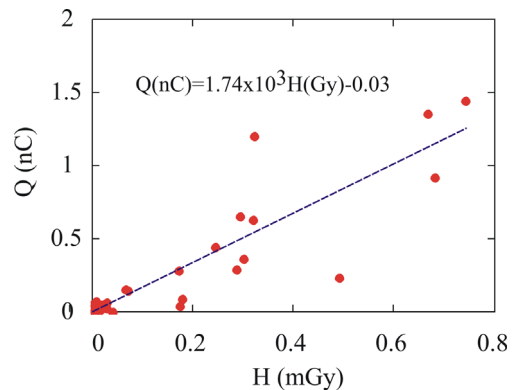
Figure 8: Comparison of BLM signal output charge with undulator magnet peak dose for a BFW01 beam strike.

[2] Corning Inc. Product Guide, "FS 7940."

[3] W. Berg et al., Proc. of LINAC08, Victoria, BC, Oct 2008, TUP043, p. 484 (2009); http://www.JACoW.org.

[4] J. M. Alderman, et al., Nucl. Instrum. Meth. A, 481 (2002) 9.

[5] B.X. Yang, private communication.

[6] A. Fasso, "Dose Absorbed in LCLS Undulator Magnets, I. Effect of a 100 μm Diamond Profile Monitor," SLAC Rad. Phys. Note, RP-05-05, May 9, 2005.